

# Analysis of Metallic Waveguides by Using Least Square-Based Finite Difference Method

C. Shu<sup>1,2</sup>, W. X. Wu<sup>2</sup> and C. M. Wang<sup>3</sup>

**Abstract:** This paper demonstrates the application of a meshfree least square-based finite difference (LSFD) method for analysis of metallic waveguides. The waveguide problem is an eigenvalue problem that is governed by the Helmholtz equation. The second order derivatives in the Helmholtz equation are explicitly approximated by the LSFD formulations. TM modes and TE modes are calculated for some metallic waveguides with different cross-sectional shapes. Numerical examples show that the LSFD method is a very efficient meshfree method for waveguide analysis with complex domains.

**keyword:** meshfree, LSFD method, metallic waveguides, eigenvalue problem, Helmholtz equation, complex domains

## 1 Introduction

The propagating characteristics of electromagnetic waves in hollow metallic conducting waveguides with general cross sections have been studied by many researchers using different numerical methods. Among them, Bulley and Davies (1969), Bulley (1970), Lin, Li, Yeo and Leong (2000a, b, 2001) have used polynomials as trial functions in the Rayleigh-Ritz method to approximate the TE and TM modes of waveguides. Thomas (1969) used trigonometric functions in polar coordinates as the trial function in the Galerkin method for solving waveguide problems. Laura, Nagaya and Sarmiento (1980) used the conformal mapping-variational approach together with the Galerkin method for analysing a waveguide with a cardioid shaped cross section.

In recent years, a generalized differential quadrature (GDQ) method was used by Shu (2000), Shu and Chew (1999), and Dong, Leong, Kooi, Lam and Shu (1997)

for solving waveguide problems. It is known that the GDQ method is a high order numerical method which yields highly accurate solutions when differential equations are solved in regular domains. For waveguides with complex cross sections, the GDQ method must be applied together with a coordinate transformation or a domain decomposition technique. This involves a tedious process in the numerical computation. The application of the traditional finite difference method (FDM) [Guan and Su (1995)] for solving waveguide problems faces the same difficulty as the GDQ method. This is because both GDQ and FDM discretize the spatial derivatives along a straight mesh line, so the domain must be regular.

To overcome the difficulties related to structured mesh point distributions, some meshfree methods have been developed in recent years. The meshfree methods make use of unstructured mesh points which can be easily placed in irregular domains and to match well with the boundaries. Examples of meshfree methods are the smooth particle hydrodynamics (SPH) method [Lucy (1977)], moving least-square (MLS) approximation [Belytschko, Gu and Lu (1994)], partition of unity methods [Duarte and Oden (1995); Belytschko, Krongauz, Organ, Fleming and Krysl (1996)], reproducing kernel particle methods (RKPM) [Liu, Chen, Uras and Chang (1996); Li and Liu (1996); Hulbert (1996); Chen, Pan, Wu and Liu (1996)], element-free Galerkin (EFG) method [Belytschko, Lu and Gu (1994)], the multiple scale finite element methods [Liu, Zhang and Ramirez (1991)], and the diffuse element method [Nayroles, Touzot and Villon (1992)].

The least square-based finite difference (LSFD) method proposed by Ding, Shu, Yeo and Xu (2004) belongs to the family of meshfree methods. Unlike most of meshfree methods, it directly solves the strong form of differential equations. The derivatives in a differential equation are directly approximated by LSFD formulations. Due to features of unstructured mesh points and the direct approximation of derivatives, the LSFD method has

<sup>1</sup> Corresponding author, Fax: +65-67791459, mpeshuc@nus.edu.sg

<sup>2</sup> Department of Mechanical Engineering, National University of Singapore

<sup>3</sup> Department of Civil Engineering, National University of Singapore, 10 Kent Ridge Crescent, Singapore 117576

the following advantages when solving the waveguide problem. One advantage is that the boundary conditions are accurately satisfied and easily implemented, and the difficulties in seeking suitable trial functions in the Rayleigh-Ritz method and the Galerkin method are completely avoided. Another advantage is that for any complex problems, numerical computation can be performed in the Cartesian coordinate system without any process for numerical integration, complicated coordinate transformation, and domain decomposition.

In this study, the Dirichlet type boundary condition is implemented by directly substituting the known function values at boundary points into the discretized governing equations. The Neumann type boundary condition is discretized and then coupled with the discretized governing equations. After implementing the boundary conditions, the Helmholtz equation can be reduced into an eigenvalue problem, in which the cutoff wavenumbers of TM and TE modes are calculated from the eigenvalues of the coefficient matrix.

## 2 Least Square-based Finite Difference (LSFD) Method and Discretization of Laplacian Operator

### 2.1 Basic LSFD formulations

In this section, we will only give a brief summary of the LSFD method. A detailed description of this method is given by Ding, Shu, Yeo and Xu (2004). For a two-dimensional (2D) function  $W(x, y)$ , Taylor series expansion in  $\Delta$  - form gives:

$$\begin{aligned} \Delta W_{ij} = & \Delta x_{ij} \frac{\partial W_i}{\partial x} + \Delta y_{ij} \frac{\partial W_i}{\partial y} + \frac{1}{2} \Delta x_{ij}^2 \frac{\partial^2 W_i}{\partial x^2} + \frac{1}{2} \Delta y_{ij}^2 \frac{\partial^2 W_i}{\partial y^2} \\ & + \Delta x_{ij} \Delta y_{ij} \frac{\partial^2 W_i}{\partial x \partial y} + \frac{1}{6} \Delta x_{ij}^3 \frac{\partial^3 W_i}{\partial x^3} + \frac{1}{6} \Delta y_{ij}^3 \frac{\partial^3 W_i}{\partial y^3} \\ & + \frac{1}{2} \Delta x_{ij}^2 \Delta y_{ij} \frac{\partial^3 W_i}{\partial x^2 \partial y} + \frac{1}{2} \Delta x_{ij} \Delta y_{ij}^2 \frac{\partial^3 W_i}{\partial x \partial y^2} + O(\Delta^4) \end{aligned} \quad (1)$$

where  $\Delta W_{ij} = W_{ij} - W_i$ ,  $\Delta x_{ij} = x_{ij} - x_i$ ,  $\Delta y_{ij} = y_{ij} - y_i$ .  $(x_i, y_i)$  are the coordinates of the point  $i$ ,  $(x_{ij}, y_{ij})$  are the coordinates of the supporting point  $ij$  around  $i$ ,  $W_i$  is the function value at the point  $i$ , and  $W_{ij}$  is the function value at the point  $ij$ ,  $\Delta$  in the truncation error is a measurement of the mean distance from the supporting points  $ij$  to the node  $i$ , for  $j = 1, 2, \dots, m$  and  $m \geq 9$ .

If we approximate the function values  $W_{ij}$  at a number of supporting points  $ij$  ( $j = 1, 2, \dots, m; m > 9$ ), and drop the

truncation errors  $O(\Delta^4)$ , we obtain a system of equations in a compact form:

$$\Delta \mathbf{W}_i = \mathbf{S}_i d\mathbf{W}_i \quad (2)$$

where

$$\Delta \mathbf{W}_i = [ \Delta W_{i1} \quad \Delta W_{i2} \quad \dots \quad \Delta W_{im} ]^T \quad (3)$$

$$d\mathbf{W}_i = \left[ \begin{array}{cccccc} \frac{\partial W_i}{\partial x} & \frac{\partial W_i}{\partial y} & \frac{\partial^2 W_i}{\partial x^2} & \frac{\partial^2 W_i}{\partial y^2} & \frac{\partial^2 W_i}{\partial x \partial y} & \\ \frac{\partial^3 W_i}{\partial x^3} & \frac{\partial^3 W_i}{\partial y^3} & \frac{\partial^3 W_i}{\partial x^2 \partial y} & \frac{\partial^3 W_i}{\partial x \partial y^2} & & \end{array} \right]^T \quad (4)$$

$$\mathbf{S}_i = \left[ \begin{array}{cccccc} \Delta x_{i1} & \Delta y_{i1} & \frac{1}{2} \Delta x_{i1}^2 & \frac{1}{2} \Delta y_{i1}^2 & \dots & \frac{1}{2} \Delta x_{i1} \Delta y_{i1}^2 \\ \Delta x_{i2} & \Delta y_{i2} & \frac{1}{2} \Delta x_{i2}^2 & \frac{1}{2} \Delta y_{i2}^2 & \dots & \frac{1}{2} \Delta x_{i2} \Delta y_{i2}^2 \\ \vdots & \vdots & \vdots & \vdots & \ddots & \vdots \\ \Delta x_{im} & \Delta y_{im} & \frac{1}{2} \Delta x_{im}^2 & \frac{1}{2} \Delta y_{im}^2 & \dots & \frac{1}{2} \Delta x_{im} \Delta y_{im}^2 \end{array} \right] \quad (5)$$

In the matrix  $\mathbf{S}_i$ , the entries are the coefficient factors of the derivatives in Taylor series expansion (1).

Now, let us define a matrix

$$\mathbf{D}_i = \text{diag} (d_i, d_i, d_i^2, d_i^2, d_i^2, d_i^3, d_i^3, d_i^3, d_i^3) \quad (6)$$

where  $d_i$  is the radius of the supporting region around the point  $i$ . We can then write

$$\Delta \mathbf{W}_i = \bar{\mathbf{S}}_i d\bar{\mathbf{W}}_i \quad (7)$$

where

$$\bar{\mathbf{S}}_i = \mathbf{S}_i \mathbf{D}_i^{-1}, d\bar{\mathbf{W}}_i = \mathbf{D}_i d\mathbf{W}_i \quad (8)$$

In equations (7), the number of equations is larger than the number of unknowns, i.e.  $m > 9$ . This is purposely done because the matrix  $\mathbf{S}_i$  is often singular or ill-conditioned at some points  $i$  in the domain  $\Omega$  when  $m = 9$ . To remove the singularity and ill-conditioned property of  $\mathbf{S}_i$ , we can use the least-squares technique to solve for  $d\bar{\mathbf{W}}_i$  from equations (7). This is equivalent to pre-multiplying the matrix  $\bar{\mathbf{S}}_i^T$  to both sides of equations (7). As a result, we have

$$\bar{\mathbf{S}}_i^T \Delta \mathbf{W}_i = \bar{\mathbf{S}}_i^T \bar{\mathbf{S}}_i d\bar{\mathbf{W}}_i \quad (9)$$

The dimensions of matrices  $\bar{\mathbf{S}}_i$  and  $\bar{\mathbf{S}}_i^T$  are  $m \times 9$  and  $9 \times m$  respectively. Hence the dimension of matrix  $\bar{\mathbf{S}}_i^T \bar{\mathbf{S}}_i$  is  $9 \times 9$ .  $m$  should be large enough to ensure that the matrix  $\bar{\mathbf{S}}_i^T \bar{\mathbf{S}}_i$  is not singular at all the points. Therefore, from equation (9), we get

$$d\bar{\mathbf{W}}_i = \left( \bar{\mathbf{S}}_i^T \bar{\mathbf{S}}_i \right)^{-1} \bar{\mathbf{S}}_i^T \Delta \mathbf{W}_i \quad (10)$$

Moreover, in order to reflect the fact that the supporting point closer to the node  $i$  has greater influence on the function value at the node  $i$ , a weighting function  $V$  is introduced in equation (10), which is then modified as follows:

$$d\bar{\mathbf{W}}_i = \left( \bar{\mathbf{S}}_i^T \mathbf{V}_i \bar{\mathbf{S}}_i \right)^{-1} \bar{\mathbf{S}}_i^T \mathbf{V}_i \Delta \mathbf{W}_i \quad (11)$$

where

$$\mathbf{V}_i = \text{diag}(V_{i1}, V_{i2}, \dots, V_{im}) \quad (12)$$

is the weighting function matrix. The following four weighting functions have been well tested by Ding, Shu, Yeo and Xu (2004):

$$1) \quad V_{ij} = \sqrt{4/\pi} (1 - \bar{r}_{ij}^2)^4, \quad (13a)$$

$$2) \quad V_{ij} = 1/\bar{r}_{ij}, \quad (13b)$$

$$3) \quad V_{ij} = 1 - 6\bar{r}_{ij}^2 + 8\bar{r}_{ij}^3 - 3\bar{r}_{ij}^4, \quad (13c)$$

$$4) \quad V_{ij} = 1/\bar{r}_{ij}^4, \quad (13d)$$

where  $\bar{r}_{ij} = \sqrt{\Delta x_{ij}^2 + \Delta y_{ij}^2} / d_i$ . It has been shown that the best accuracy of the numerical results can be obtained by using the weighting function (13a) rather than (13b-d). Therefore, in our study, (13a) is adopted for solving the waveguide problems. The final LSFDF formulations can be derived from equations (8) and (11) as

$$d\mathbf{W}_i = \mathbf{D}_i^{-1} \left( \bar{\mathbf{S}}_i^T \mathbf{V}_i \bar{\mathbf{S}}_i \right)^{-1} \bar{\mathbf{S}}_i^T \mathbf{V}_i \Delta \mathbf{W}_i \quad (14)$$

In order to simplify this formulation, we can define matrix  $\mathbf{T}^i$  as

$$\mathbf{T}^i = \mathbf{D}_i^{-1} \left( \bar{\mathbf{S}}_i^T \mathbf{V}_i \bar{\mathbf{S}}_i \right)^{-1} \left( \bar{\mathbf{S}}_i^T \mathbf{V}_i \right) \quad (15)$$

Then formulation (14) can be rewritten as

$$d\mathbf{W}_i = \mathbf{T}^i \Delta \mathbf{W}_i \quad (16)$$

where  $\Delta \mathbf{W}_i$  and  $d\mathbf{W}_i$  are vectors given by expressions (3) and (4), respectively, and  $\mathbf{T}^i \in R^{9 \times m}$ .

From the forgoing process, we can see that the LSFDF formulation (F-9) is derived by using the 2D Taylor series expansion with the first nine truncated terms. We can also derive higher order LSFDF schemes which approximate derivatives of a function with higher order of accuracy by using the 2D Taylor series expansions with more truncated terms. For easy reference, we denote the LSFDF formulation derived by using 2D Taylor series expansion with the first 14 truncated terms by (F-14).

## 2.2 LSFDF formulation for $\nabla^2 W_i$

The Helmholtz equation for eigenvalue problems can be written as

$$\nabla^2 W = -k^2 W \quad (17)$$

where the Laplacian operator is defined by

$$\nabla^2 = \frac{\partial^2}{\partial x^2} + \frac{\partial^2}{\partial y^2} \quad (18)$$

From formulation (16) and expression (18), we have

$$\begin{aligned} \nabla^2 W_i &= \sum_{j=1}^m [\mathbf{T}_{3,j}^i + \mathbf{T}_{4,j}^i] \Delta W_{ij} \\ &= \sum_{j=1}^m [\mathbf{T}_{3,j}^i + \mathbf{T}_{4,j}^i] W_{ij} + \left\{ - \sum_{j=1}^m [\mathbf{T}_{3,j}^i + \mathbf{T}_{4,j}^i] \right\} W_i \end{aligned} \quad (19)$$

We can define a vector  $\bar{\mathbf{T}}^i$  by giving its elements as

$$\bar{\mathbf{T}}_j^i = \mathbf{T}_{3,j}^i + \mathbf{T}_{4,j}^i \quad \text{for } j = 1, 2, \dots, m. \quad (20)$$

Then equation (19) can be simplified to

$$\nabla^2 W_i = \sum_{j=1}^m \bar{\mathbf{T}}_j^i \Delta W_{ij} = \sum_{j=1}^m \bar{\mathbf{T}}_j^i W_{ij} + \left[ - \sum_{j=1}^m \bar{\mathbf{T}}_j^i \right] W_i \quad (21)$$

Therefore the Helmholtz equation (17) can be discretized as

$$\sum_{j=1}^m \bar{\mathbf{T}}_j^i W_{ij} + \left[ - \sum_{j=1}^m \bar{\mathbf{T}}_j^i \right] W_i = -k^2 W_i \quad \text{for } i = 1, 2, \dots, n \quad (22)$$

### 3 Eigenvalue problems of Helmholtz equation

#### 3.1 Definition of the problem

In telecommunications, a waveguide is a material medium that confines and guides a propagating electromagnetic wave. In the microwave regime, a waveguide normally consists of a hollow metallic conductor, usually rectangular, elliptical, or circular in cross section. The propagation characteristics of hollow metallic conducting waveguides with homogeneous permittivity and permeability distributions can be fully defined by the Helmholtz equation

$$\nabla^2 \phi = -k_c^2 \phi \text{ in } \Omega \tag{23}$$

where  $k_c$  is the cutoff wavenumber, and  $\phi$  the longitudinal component of electric or magnetic field defined in the two-dimensional domain  $\Omega$  surrounded by the boundary  $\Gamma$ . There are two types of guiding modes, namely TM modes and TE modes, and their boundary conditions are

$$\phi = 0 \text{ at } \Gamma \text{ for TM modes,} \tag{24}$$

$$\frac{\partial \phi}{\partial n} = 0 \text{ at } \Gamma \text{ for TE modes.} \tag{25}$$

#### 3.2 Numerical discretization by LSFDF

At first, we need to generate  $n_T$  nodal points  $(x_i, y_i)$ ,  $i = 1, 2, \dots, n_T$  in domain  $\Omega$ . There are  $n_i$  interior points and  $n_b = n_T - n_i$  boundary points. For curved boundaries, we also need to define  $\theta_i$ ,  $i = n_i + 1, n_i + 2, \dots, n_T$ , which is the angle between the positive  $x$ -axis and the normal vector  $\mathbf{n}_i$  at the boundary point  $i$ .

Based on the node distribution in the domain  $\Omega$ , we generate a data file in which the global ordinal numbers of  $m$  nearest supporting points around the node  $i$  ( $i = 1, 2, \dots, n_T$ ) are given as  $ij$  ( $j = 1, 2, \dots, m$ ). The radius  $d_i$  of the supporting region associated to the node  $i$  is calculated by

$$d_i = \max \left\{ \sqrt{(x_{ij} - x_i)^2 + (y_{ij} - y_i)^2} \right\} \times 1.2 \tag{26}$$

for  $j = 1, 2, \dots, m$ ; and  $i = 1, 2, \dots, n_T$ . The matrices  $\mathbf{T}^i$  ( $i = 1, 2, \dots, n_T$ ) are calculated by using the formulation (15), and the vectors  $\bar{\mathbf{T}}^i$  ( $i = 1, 2, \dots, n_T$ ) are calculated by using the formulation (19).

With all the above data available, and by using the formulation (21), we can discretize the Helmholtz equation (22) at each interior point as

$$\sum_{j=1}^m \bar{\mathbf{T}}_j^i \phi_{ij} + \left[ - \sum_{j=1}^m \bar{\mathbf{T}}_j^i \right] \phi_i = -k_c^2 \phi_i \text{ for } i = 1, 2, \dots, n_i \tag{27}$$

In equation (26), there are  $n_i$  equations in which  $\phi_i$  ( $i = 1, 2, \dots, n_i$ ) and  $\phi_{ij}$  ( $1 \leq ij \leq n_T$ ) are unknowns. So there are  $n_T$  unknowns. For the TM modes, the boundary condition is

$$\phi_i = 0 \text{ for } i = n_i + 1, n_i + 2, \dots, n_T \tag{28}$$

By substituting (27) into equation (26), the number of unknowns can be reduced to  $n_i$  which is equal to the number of equations, and equation (26) can be reduced to a matrix-vector form as

$$\mathbf{A} \mathbf{a} = -k_c^2 \mathbf{a} \tag{29}$$

where the coefficient matrix  $\mathbf{A} \in R^{n_i \times n_i}$ , the vector  $\mathbf{a} = [\phi_1, \phi_2, \dots, \phi_{n_i}]^T$ . The cutoff wavenumbers  $k_c$  for TM modes can be obtained by calculating the eigenvalues of the matrix  $\mathbf{A}$ .

For TE modes, the boundary condition is

$$\frac{\partial \phi_i}{\partial n} = 0 \text{ for } i = n_i + 1, n_i + 2, \dots, n_T \tag{30}$$

which is equivalent to

$$\frac{\partial \phi_i}{\partial x} \cos \theta_i + \frac{\partial \phi_i}{\partial y} \sin \theta_i = 0 \text{ for } i = n_i + 1, n_i + 2, \dots, n_T \tag{31}$$

Using the formulation (F-9), we can discretize equation (31) as

$$\sum_{j=1}^m \{ \mathbf{T}_{1,j}^i \cos \theta_i + \mathbf{T}_{2,j}^i \sin \theta_i \} \phi_{ij} + \left\{ \left[ - \sum_{j=1}^m \mathbf{T}_{1,j}^i \right] \cos \theta_i + \left[ - \sum_{j=1}^m \mathbf{T}_{2,j}^i \right] \sin \theta_i \right\} \phi_i = 0 \tag{32}$$

for  $i = n_i + 1, n_i + 2, \dots, n_T$ . By moving all the terms which contain the function values at interior points,  $\phi_{ij}$

( $ij \leq n_i$ ), from left-hand side to right-hand side, equations (32) can be compactly expressed as

$$\mathbf{B}\mathbf{a}_b = \mathbf{C}\mathbf{a} \quad (33)$$

where the vectors  $\mathbf{a}_b = [\phi_{n_i+1}, \phi_{n_i+2}, \dots, \phi_{n_T}]^T$ ,  $\mathbf{a} = [\phi_1, \phi_2, \dots, \phi_{n_i}]^T$ , the matrix  $\mathbf{B} \in \mathbb{R}^{n_b \times n_b}$ , and the matrix  $\mathbf{C} \in \mathbb{R}^{n_b \times n_i}$ . Equation (33) can be further reduced to

$$\mathbf{a}_b = \mathbf{B}^{-1}\mathbf{C}\mathbf{a} \quad (34)$$

From equation (34) we have

$$\phi_{n_i+k} = \sum_{l=1}^{n_i} (\mathbf{B}^{-1}\mathbf{C})_{k,l} \phi_l, \text{ for } k = 1, 2, \dots, n_b \quad (35)$$

Equation (35) implies that the function value at each boundary point can be expressed as a linear combination of the function values at all the interior points. By substituting equation (35) into equations (26), we can reduce the system of discretized governing equation (26) into the matrix-vector form which is the same as equation (29), and the cutoff wavenumbers  $k_c$  for TE modes can be obtained from the eigenvalues of the matrix  $\mathbf{A}$ . In this study, the eigenvalues of matrices are computed by using HBG and HQR subroutines provided by Xu (1995).

### 3.2.1 Dealing with singular points on the boundary $\Gamma$

For the TE modes, the boundary condition is given by either equation (30) or (31), i.e.

$$\frac{\partial \phi_i}{\partial n} = 0 \text{ or } \frac{\partial \phi_i}{\partial x} \cos \theta_i + \frac{\partial \phi_i}{\partial y} \sin \theta_i = 0 \quad (36)$$

for  $i = n_i + 1, n_i + 2, \dots, n_T$ . It is noted that some boundary points may be located at the sharp corner where the normal vector  $\mathbf{n}_i$  and the angle  $\theta_i$  are not unique. Obviously, these points are singular positions. The way in dealing with singular points may affect the accuracy of numerical results sensitively when the boundary condition (35) is implemented. Basically, there are two types of singular points on the boundary  $\Gamma$ , namely the convex-type singular points where the domain  $\Omega$  is convex, and the concave-type singular points where the domain  $\Omega$  is concave (Fig. 1). We found that the concave-type singular points need to be handled specially, so that the accurate solutions of the TE modes can be obtained. In this work, all concave-type singular points need to be eliminated from the supporting points of any node  $i$ .

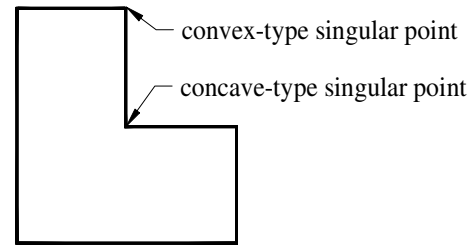


Figure 1 : Singular points on the boundary  $\Gamma$

## 3.3 Results and discussion

The LSF method is validated by its application in solving a set of waveguide problems. At first, the LSF results for TE modes of a rectangular waveguide are computed and compared with the analytical solution. Then it is applied to compute the cutoff wavenumbers of the TM and TE modes for the double-ridged, L-shaped, single-ridged, coaxial rectangular, and vane rectangular waveguides. The LSF results are compared with available data in the literature. It is noted that for all the cases, when the TE modes are considered, there is a null mode with the cutoff wavenumber being zero in the LSF results. However, this null mode does not exist physically and is removed from the tables. The same results regarding the null mode for the TE modes have also been reported by Shu and Chew (1999).

### 3.3.1 Rectangular waveguide

Consider a rectangular waveguide as shown in Fig. 2. The cutoff wavenumbers of the TE modes are computed by the LSF method and then compared with the analytical solution which can be expressed by

$$k_c = \pi \sqrt{(m/a)^2 + (n/b)^2}, \quad m, n = 0, 1, 2, \dots \quad (37)$$

For the LSF computation, we generated 2232 and 3341 unstructured nodal points in the rectangular domain respectively. The numerical results are obtained for the following three cases: Case 1,  $n_T = 2232$  and the formulation (F-9) is applied; Case 2,  $n_T = 2232$  and the formulation (F-14) which is one order higher in accuracy than (F-9) is applied; Case 3,  $n_T = 3341$  and the formulation (F-9) is applied. Tab. 1 shows the computed LSF cutoff wavenumbers of the first ten TE modes for the three cases and the corresponding absolute errors from the analytical solution.

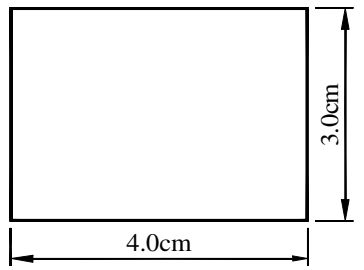


Figure 2 : Configuration of a rectangular waveguide

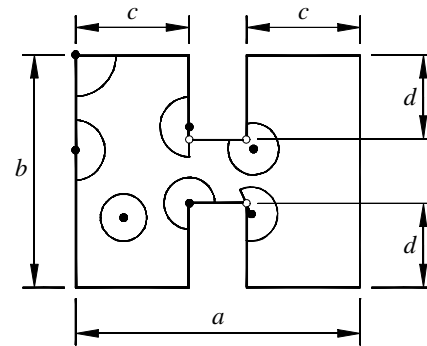


Figure 3 : Configuration of a double-ridged waveguide

Analytical Solution	LSFD Results			Absolute Errors		
	Case 1	Case 2	Case 3	Case 1	Case 2	Case 3
0.785398163	0.785183102	0.785397819	0.785253625	$2.151 \times 10^{-4}$	$3.440 \times 10^{-7}$	$1.445 \times 10^{-4}$
1.047197551	1.046672419	1.047195430	1.046858483	$5.251 \times 10^{-4}$	$2.121 \times 10^{-6}$	$3.391 \times 10^{-4}$
1.308996939	1.308074232	1.308992910	1.308375527	$9.227 \times 10^{-4}$	$4.029 \times 10^{-6}$	$6.214 \times 10^{-4}$
1.570796327	1.569061476	1.570789926	1.569641063	$1.735 \times 10^{-3}$	$6.401 \times 10^{-6}$	$1.155 \times 10^{-3}$
1.887862233	1.885101160	1.887842833	1.886036557	$2.761 \times 10^{-3}$	$1.940 \times 10^{-5}$	$1.826 \times 10^{-3}$
2.094395102	2.090224697	2.094351927	2.091655246	$4.170 \times 10^{-3}$	$4.318 \times 10^{-5}$	$2.740 \times 10^{-3}$
2.236814950	2.232042601	2.236769472	2.233605533	$4.772 \times 10^{-3}$	$4.548 \times 10^{-5}$	$3.209 \times 10^{-3}$
2.356194490	2.350346339	2.356133055	2.352304817	$5.848 \times 10^{-3}$	$6.144 \times 10^{-5}$	$3.890 \times 10^{-3}$
2.578424943	2.571248493	2.578340608	2.573652265	$7.176 \times 10^{-3}$	$8.434 \times 10^{-5}$	$4.773 \times 10^{-3}$
2.617993878	2.610793045	2.617920988	2.613106773	$7.201 \times 10^{-3}$	$7.289 \times 10^{-5}$	$4.887 \times 10^{-3}$

Table 1 : Analytical and LSFD results of TE modes of the rectangular waveguide: Case 1:  $n_T = 2232$ , (F - 9); Case 2:  $n_T = 2232$ , (F - 14); Case 3:  $n_T = 3341$ , (F - 9)

Approaches	Meshes	$TE_1$	$TE_3$	$TE_5$	$TE_7$	$TE_9$
LSFD	3252, (F-9)	1.4307	3.1608	6.1827	6.7045	6.9601
	3252, (F-14)	1.4426	3.1654	6.1906	6.7178	6.9727
M-D GDQ	$19 \times 19$	1.4423	3.1684	6.1917	6.7127	6.9757
FD-SIC	$50 \times 40$	1.428	3.169	6.192	6.695	6.976
	$100 \times 80$	1.434	3.168	6.192	6.705	6.975
Montgomery		1.437	3.166	6.190	6.712	6.973
Utsumi		1.438	3.155	6.215	6.707	6.971
Scalar-FEM		1.440	-	6.192	6.713	-

Table 2 : Cutoff wavenumbers for the double-ridged waveguide

It was found that the computing time of present calculation takes about 1% for forming the coefficient matrix **A** and 99% for calculating the eigenvalues of matrix **A**. The time taken for calculating the eigenvalues of a matrix depends on the dimension of the matrix. As shown

in Tab. 1, Case 1 provides the LSFD results with reasonable accuracy. The absolute errors of Case 3 are reduced by about one-third as compared to Case 1. Clearly, its improvement in accuracy of solution is moderate, but its computing time is increased from 1 hour required by

Mesh	LSFD		M-D GDQ	FD-SIC	FD-CGM	SIE
	3570, (F-9)	3570, (F-14)	$21 \times 21$			
$TM_1$	4.8839	4.8927	4.8902	4.8949	4.80	4.8677
$TM_2$	6.1326	6.1391	6.1392	6.1350	6.07	6.1361
$TM_3$	6.9872	6.9966	6.9967	6.9921	6.92	6.9908
$TM_4$	8.5391	8.5564	8.5565	8.5458	8.61	8.5525
$TM_5$	8.8734	8.8994	8.8972	8.8940	9.72	-
$TM_6$	10.1108	10.1439	10.1425	10.1262	11.39	-
$TM_7$	10.5253	10.5577	10.5580	10.5318	-	-
$TM_8$	11.0252	11.0625	11.0627	11.0380	-	-
$TM_9$	11.0254	11.0625	11.0627	11.0380	-	-
$TM_{10}$	11.8114	11.8608	11.8598	11.8407	-	-
$TE_1$	1.9141	1.9165	1.9123	1.9111	-	1.8917
$TE_2$	2.9602	2.9605	2.9605	2.9600	-	2.9159
$TE_3$	4.9439	4.9474	4.9474	4.9452	-	4.8755
$TE_4$	4.9440	4.9474	4.9474	4.9452	-	-
$TE_5$	5.3110	5.3147	5.3147	5.3128	-	5.2463
$TE_6$	5.5807	5.5877	5.5831	5.5799	-	-
$TE_7$	6.9880	6.9966	6.9967	6.9937	-	-
$TE_8$	7.2813	7.2963	7.2879	7.2784	-	-
$TE_9$	7.5982	7.6088	7.6088	7.6002	-	-
$TE_{10}$	8.3931	8.4124	8.4045	-	-	-

**Table 3** : Cutoff wavenumbers of the L-shaped waveguide

Case 1 to 2.5 hours on a Fujitsu Pentium 4 notebook computer. In contrast, the absolute errors of Case 2 are only about 0.73% of those of Case 1, but its computing time required is almost the same as Case 1. This is because Cases 1 and 2 use the same total number of points,  $n_T = 2232$ . So, the dimension of coefficient matrix for these two cases is the same, and thus the computing time required for calculating the eigenvalues is also the same. On the other hand, the formulation (F-14) used by Case 2 has one order higher in accuracy than the formulation (F-9) used by Case 1. Therefore, the results of Case 2 are much more accurate than those of Case 1. Both Case 3 and Case 1 have the same order of accuracy since they use the same formulation (F-9). The improvement of numerical results in Case 3 is actually due to the reduction of distance between points when the total number of points is increased from  $n_T = 2232$  to  $n_T = 3341$ . On the other hand, since the dimension of the coefficient matrix in Case 3 is larger than that in Case 1, Case 3 would definitely need more computing time. The above results also imply that the accuracy of numerical results can be more efficiently improved by increasing the order of accuracy

for derivative approximation.

### 3.3.2 Double-Ridged waveguide

The geometry of the cross section of a double-ridged waveguide is shown in Fig. 3. For this problem, the domain  $\Omega$  is non-convex. As discussed in the sub-section 3.2.1, the four singular concave points on  $\Gamma$  cannot be appointed as the supporting points of other nodes. Some typical supporting regions are shown in Fig. 3. The principle for the selection of supporting region is that the line segment between a node and its supporting point should not be outside the domain  $\Omega$ .

The cutoff wavenumbers for  $TE_1$ ,  $TE_3$ ,  $TE_5$ ,  $TE_7$  and  $TE_9$  modes are computed by the LSFD method, and then compared with the available results from other methods [Guan and Su (1995); Shu and Chew (1999); Montgomery (1971); Utsumi (1985); Israel and Min-iowitz (1987)] in Tab. 2. Clearly the present results agree very well with those obtained from other methods. The results based on (F-14) formulation are much more accurate than those based on (F-9) formulation.

### 3.3.3 L-Shaped waveguide

The geometry of the L-shaped waveguide is shown in Fig. 4. Tab. 3 shows the computed cutoff wavenumbers of the first ten TM and TE modes by LSFD method for this waveguide. Also included in Tab. 3 are the results of the multi-domain GDQ method [Shu and Chew (1999)], the surface integral equation (SIE) method [Swaminathan, Arvas, Sarkar and Djordjevic (1990)], the finite difference with conjugate gradient method (FD-CGM) [Sarkar, Athar, Arvas, Manela and Lade (1989)], and the FD-SIC method [Guan and Su (1995)]. As shown by Guan and Su (1995), analytical solutions for  $TM_3$ ,  $TM_8$ ,  $TM_9$ ,  $TE_3$ ,  $TE_4$ ,  $TE_7$  modes are available, and their respective values are 6.9967, 11.0627, 11.0627, 4.9474, 4.9474, and 6.9967. From Tab. 3, we can see that the multi-domain GDQ results are very accurate, and the LSFD results based on formulation (F-14) are much closer to the multi-domain GDQ results than those based on formulation (F-9). This indicates that the LSFD results can be improved more effectively by increasing the order of accuracy of the formulation used.

### 3.3.4 Single-Ridged waveguide

The configuration of a single-ridged waveguide is shown in Fig. 5. Tab. 4 shows the computed cutoff wavenumbers of the first ten TM and TE modes by LSFD method for this waveguide. Also included in this table are the results obtained from the multi-domain GDQ method [Shu and Chew (1999)], the SIE method [Swaminathan, Arvas, Sarkar and Djordjevic (1990)], the FD-CGM method [Sarkar, Athar, Arvas, Manela and Lade (1989)], and the FD-SIC method [Guan and Su (1995)]. The results of LSFD method are reasonably accurate as compared with those of the multi-domain GDQ method. Again, the accuracy of LSFD results can be improved considerably when the formulation (F-14) rather than the formulation (F-9) is used to approximate the derivatives in the Helmholtz equation (22) and the boundary condition equation (31).

### 3.3.5 Coaxial Rectangular waveguide

The configuration of a coaxial rectangular waveguide is shown in Fig. 6. Tab. 5 shows the computed cutoff wavenumbers of the first ten TM and TE modes by LSFD method for this problem. Also included in Tab. 5 are the results of the multi-domain GDQ method [Shu and Chew (1999)] and the FD-CGM method [Sarkar, Athar, Arvas,

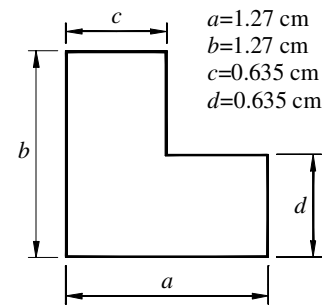


Figure 4 : Configuration of a L-shaped waveguide

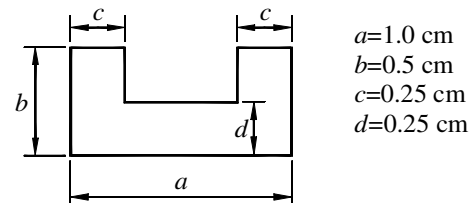


Figure 5 : Configuration of a single-ridged waveguide

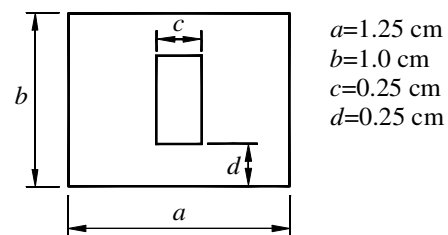


Figure 6 : Configuration of a coaxial waveguide

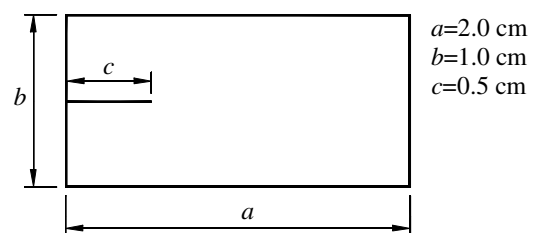


Figure 7 : Configuration of a vaned rectangular waveguide

Manela and Lade (1989)]. Clearly, the results of TM and TE modes of LSFD method are compared well with those of the multi-domain GDQ method.

### 3.3.6 Vaned Rectangular waveguide

The configuration of a vaned rectangular waveguide is shown in Fig. 7 and the computed cutoff wavenumbers



Mesh	LSFD		M-D GDQ	FD-SIC	FD- CGM	SIE
	2021, (F-9)	2021, (F-14)	21×21			
$TM_1$	12.0946	12.1432	12.1362	12.1447	12.05	12.0381
$TM_2$	12.3748	12.4296	12.4210	12.4331	12.32	12.2938
$TM_3$	13.9633	14.0101	14.0090	14.0037	13.86	13.9964
$TM_4$	15.5327	15.5917	15.5935	15.5829	15.34	15.5871
$TM_5$	16.5778	16.6495	16.6507	16.6403	16.28	-
$TM_6$	17.6841	17.7709	17.7715	17.7598	-	-
$TM_7$	19.5250	19.6434	19.6447	19.6296	19.32	-
$TM_8$	21.5738	21.7318	21.7335	21.0763	-	-
$TM_9$	22.0983	22.2873	22.2838	-	-	-
$TM_{10}$	22.3966	22.6061	22.5990	-	-	-
$TE_1$	2.2583	2.2580	2.2489	2.2422	2.23	2.2496
$TE_2$	4.8683	4.8731	4.8573	4.8543	4.78	4.9436
$TE_3$	6.4573	6.4664	6.4548	6.4476	6.40	6.5189
$TE_4$	7.5200	7.5187	7.5196	7.5185	7.48	7.5642
$TE_5$	9.8151	9.8217	9.8254	9.8314	9.71	-
$TE_6$	12.5345	12.5659	12.5664	12.5607	12.39	-
$TE_7$	12.5353	12.5660	12.5664	12.5607	-	-
$TE_8$	12.7500	12.7832	12.7785	12.7667	-	-
$TE_9$	13.3505	13.3817	13.3818	13.3825	-	-
$TE_{10}$	13.4687	13.4981	13.4993	-	-	-

**Table 4 :** Cutoff wavenumbers of the single-ridged waveguide

of the first ten TM and TE modes by LSF method are displayed in Tab. 6 for this waveguide. Tab. 6 also includes the results of the multi-domain GDQ method [Shu and Chew (1999)], the FD-CGM method [Sarkar, Athar, Arvas, Manela and Lade (1989)] and the SIE method [Swaminathan, Arvas, Sarkar and Djordjevic (1990)]. Like other cases, the LSF results of TM and TE modes for this case also agree well with available results in the literature.

#### 4 Conclusions

In this paper, we have presented the recently developed LSF meshfree method for solving eigenvalue problems governed by the Helmholtz equation. Through this study, we can see that the LSF method can be efficiently used to solve waveguide problems within complex domains. For any geometry, the strong form of differential equations is directly discretized by the LSF formulations and solved in the Cartesian coordinate system without the need for any coordinate transformation or domain decomposition. The boundary conditions of TM modes and

TE modes are implemented easily. For all the waveguide problems dealt in the paper, the LSF results show good accuracy. It is also established that the accuracy of the numerical results can be improved by using higher order LSF formulations rather than by increasing the total number of points in the problem domain.

#### References

- Belytschko, T.; Gu, L.; Lu, Y. Y.** (1994): Fracture and crack growth by element-free Galerkin method. *Model. Simul. Mater. Sci. Engrg.* 2, pp. 519-534.
- Belytschko, T.; Krongauz, Y.; Organ, D.; Fleming, M.; Krysl, P.** (1996): Meshless methods: An overview and recent developments. *Comput. Methods Appl. Mech. Engrg.*, vol. 139, 1996, pp. 3-47.
- Belytschko, T.; Lu, Y. Y.; Gu, L.** (1994): Element free Galerkin methods. *Int. J. Numer. Meth. Engrg.*, vol. 37, pp. 229-256.
- Bulley, R. M.** (1970): Analysis of the arbitrarily shaped waveguide by polynomial approximation. *IEEE Trans.*

Meshes	LSFD		M-D GDQ	FD-CGM
	3409, (F-9)	3409, (F-14)	17×17	
$TM_1$	6.9297	6.9438	6.9387	6.91
$TM_2$	6.9406	6.9543	6.9497	6.96
$TM_3$	8.6347	8.6622	8.6514	8.50
$TM_4$	8.6760	8.7024	8.6932	8.51
$TM_5$	10.8838	10.9313	10.9176	10.57
$TM_6$	11.0206	11.0652	11.0564	10.83
$TM_7$	12.4492	12.5273	12.4994	-
$TM_8$	12.4735	12.5412	12.5253	-
$TM_9$	12.6645	12.7316	12.7198	-
$TM_{10}$	13.1145	13.1978	13.1737	-
$TE_1$	1.8865	1.8987	1.8900	1.85
$TE_2$	2.8372	2.8330	2.8281	2.81
$TE_3$	3.9124	3.9169	3.9108	3.89
$TE_4$	5.1415	5.1419	5.1410	5.05
$TE_5$	5.7474	5.7495	5.7516	5.68
$TE_6$	6.3408	6.3526	6.3543	6.25
$TE_7$	6.3474	6.3601	6.3612	-
$TE_8$	7.0382	7.0523	7.0451	-
$TE_9$	7.8943	7.9133	7.9010	-
$TE_{10}$	8.1551	8.1800	8.1740	-

**Table 5** : Cutoff wavenumbers of the coaxial rectangular waveguide

*Microwave Theory Tech.*, MTT-18, No.12, pp. 1022-1028.

**Bulley, R. M.; Davies, J. B.** (1969): Computation of approximate polynomial solutions to TE modes in an arbitrarily shaped waveguide. *IEEE Trans. Microwave Theory Tech.*, MTT-17, No.8, pp. 440-446.

**Chen, J. S.; Pan, C. H.; Wu, C. T.; Liu, W. K.** (1996): Reproducing kernel particle methods for large deformation analysis of non-linear structures. *Comput. Methods Appl. Mech. Engrg.*, vol. 139, pp. 195-227.

**Ding, H.; Shu, C.; Yeo, K. S.; Xu, D.** (2004): Development of least square-based two-dimensional finite difference schemes and their application to simulate natural convection in a cavity. *Computers & Fluids*, vol. 33, pp. 137-154.

**Dong, Y. C.; Leong, M. S.; Kooi, P. S.; Lam, K. Y.; Shu, C.** (1997): Computation of the propagation characteristics of TE and TM modes in waveguides with the use of the generalized differential quadrature method. *Microwave and Optical Technology Letters*, vol. 14, No.1, pp. 39-44.

**Duarte, C. A.; Oden, J. T.** (1995): *Hp* clouds—a meshless method to solve boundary-value problems, Technical Report 95-05. Texas Institute for Computational and Applied Mathematics, University of Texas at Austin.

**Guan, J. M.; Su, C. C.** (1995): Analysis of metallic waveguides with rectangular boundaries by using the finite-difference method and the simultaneous iteration with the Chebyshev acceleration. *IEEE Trans. Microwave Theory Tech.*, MTT-43, pp. 374-382.

**Hulbert, G. M.** (1996): Application of reproducing kernel particle methods in electromagnetics. *Comput. Methods Appl. Mech. Engrg.*, vol. 139, pp. 229-235.

**Israel, M.; Miniowitz, R.** (1987): An efficient finite method for nonconvex waveguide based on hermitian polynomials. *IEEE Trans. Microwave Theory Tech.*, MTT-35, pp. 1019-1026.

**Laura, P. A. A.; Nagaya, K.; Sarmiento, G. S.** (1980): Numerical experiments on the determination of cutoff frequencies of waveguides of arbitrary cross section. *IEEE Trans. Microwave Theory Tech.*, MTT-28, No.6, pp. 568-572.

	LSFD		M-D GDQ	FD-CGM	SIE
Meshes	2691, (F-9)	2691, (F-14)	23×23		
$TM_1$	3.6902	3.6967	3.6932	3.65	3.6770
$TM_2$	4.9652	4.9823	4.9726	4.87	4.9279
$TM_3$	6.4555	6.4765	6.4721	6.31	6.4151
$TM_4$	6.4600	6.4849	6.4766	7.59	-
$TM_5$	7.0035	7.0247	7.0248	8.65	7.0220
$TM_6$	7.7135	7.7449	7.7428	9.29	-
$TM_7$	7.8239	7.8538	7.8540	-	-
$TM_8$	8.8394	8.8853	8.8831	-	-
$TM_9$	8.8420	8.8877	8.8858	-	-
$TM_{10}$	9.5787	9.6332	9.6328	-	-
$TE_1$	1.5493	1.5591	1.5698	1.57	1.5695
$TE_2$	2.0850	2.0784	2.0805	2.00	2.1156
$TE_3$	3.1427	3.1464	3.1390	3.13	3.1568
$TE_4$	3.3013	3.3035	3.3036	3.28	3.3046
$TE_5$	4.2456	4.2500	4.2500	4.23	-
$TE_6$	4.7303	4.7288	4.7083	4.66	-
$TE_7$	5.4935	5.5028	5.5020	-	-
$TE_8$	6.2675	6.2830	6.2781	-	-
$TE_9$	6.2681	6.2831	6.2832	-	-
$TE_{10}$	6.4499	6.4711	6.4758	-	-

**Table 6 :** Cutoff wavenumbers of the vaned rectangular waveguide

- Li, S. F.; Liu, W. K.** (1996): Moving least-square reproducing kernel method Part II: Fourier analysis. *Comput. Methods Appl. Mech. Engrg.*, vol. 139, pp. 159-193.
- Lin, S. L.; Li, L. W.; Yeo, T. S.; Leong, M. S.** (2000a): Analysis of hollow conducting waveguides using superquadric functions—A unified representation. *IEEE Trans. Microwave Theory Tech.*, vol. 48, No.5, pp. 876-880.
- Lin, S. L.; Li, L. W.; Yeo, T. S.; Leong, M. S.** (2000b): QZ factorization for generalized eigenvalues applied to waveguide analysis. *Microwave and Optical Technology Letters*, vol. 28, No.5, pp. 361-364.
- Lin, S. L.; Li, L. W.; Yeo, T. S.; Leong, M. S.** (2001): Analysis of metallic waveguides of a large class of cross sections using polynomial approximation and superquadric functions. *IEEE Trans. Microwave Theory Tech.*, vol. 49, No.6, pp. 1136-1139.
- Liu, W. K.; Chen, Y. J.; Uras, R. A.; Chang, C. T.** (1996): Generalized multiple scale reproducing kernel particle methods. *Comput. Methods Appl. Mech. Engrg.*, vol. 139, pp. 91-157.
- Liu, W. K.; Zhang, Y.; Ramirez, M. R.** (1991): Multiple scale finite element methods. *Int. J. Numer. Meth. Engrg.*, vol. 32, pp. 969-990.
- Lucy, L. B.** (1977): A numerical approach to the testing of the fission hypothesis. *The Astron. J.* 8(12), pp. 1013-1024.
- Nayroles, B.; Touzot, G.; Villon, P.** (1992): Diffuse approximation and diffuse elements. *Comput. Mech.*, vol. 10, pp. 307-318.
- Montgomery, J. P.** (1971): On the complete eigenvalue solution of ridged waveguide. *IEEE Trans. Microwave Theory Tech.*, MTT-19, pp. 547-555.
- Sarkar, T. K.; Athar, K.; Arvas, E.; Manela, M.; Lade, R.** (1989): Computation of the propagation characteristics of TE and TM modes in arbitrarily shaped hollow waveguides utilizing the conjugate gradient method. *J. Electromagn. Waves Appl.*, vol. 3, pp. 143-165.
- Shu, C.** (2000): Analysis of elliptical waveguides by differential quadrature method. *IEEE Trans. Microwave Theory Tech.*, 48, No.2, pp. 319-322.

**Shu, C.; Chew, Y. T.** (1999): Application of multi-domain GDQ method to analysis of waveguides with rectangular boundaries. *Progress In Electromagnetics Research*, PIER 21, pp. 1-19.

**Swaminathan, M.; Arvas, E.; Sarkar, T. K.; Djordjevic, A. R.** (1990): Computation of cutoff wavenumbers of TE and TM modes in waveguides of arbitrary cross sections using a surface integral formulation. *IEEE Trans. Microwave Theory Tech.*, MTT-38, pp. 154-159.

**Thomas, D. T.** (1969): Functional approximations for solving boundary value problems by computer. *IEEE Trans. Microwave Theory Tech.*, MTT-17, No.8, pp. 447-454.

**Utsumi, Y.** (1985): Variational analysis of ridged waveguide mode. *IEEE Trans. Microwave Theory Tech.*, MTT-33, 1985, pp. 111-120.

**Xu, S. L.** (1995): *Fortran programs for common algorithms. Second edition (in Chinese)*, Qinghua University Press.